Proceedings of ASME Turbo Expo 2020: Turbomachinery Technical Conference and Exposition
GT2020
June 22 – 26, 2020, London, United Kingdom

GT2020–14564

EXPERIMENTAL INVESTIGATION OF THE COMBUSTION BEHAVIOR OF SINGLE–NOZZLE LIQUID–FLOX®–BASED BURNERS ON AN ATMOSPHERIC TEST RIG

Saeed Izadi, Jan Zanger, Oliver Kislat, Benedict Enderle, Felix Grimm, Peter Kutne, Manfred Aigner

German Aerospace Center (DLR), Institute of Combustion Technology
D–70569 Stuttgart, Germany
Email: saeed.izadi@dlr.de

ABSTRACT

As an alternative to the commonly used swirl burners in micro gas turbines (MGT), the FLOX®–based combustion concept promises great potential for the nitric oxide emission reduction and increased fuel flexibility. Previous research on FLOX®–based MGT combustors mainly addressed gaseous fuels and there is limited knowledge available on liquid fuel FLOX®–based MGT combustors. Despite having to deal with a new set of challenges while utilizing liquid fuel in the burner, first steps are taken to gain more information on the influencing operational parameters. In this regard, a FLOX®–based liquid fuel burner is developed to fit into a newly designed combustor for the Capstone C30 MGT. The C30 combustor operates with three burners arranged tangentially to an annular combustion chamber and provides a total thermal power of 115 kW. In this work, operational properties of merely one of the three C30 liquid fuel burners are investigated and the rest of the two burners are emulated in form of hot cross–flow. As for the liquid burners, the experiments are conducted with three geometrically different single–nozzle burners at atmospheric pressure. The studied FLOX®–based burners consist of an air nozzle with a coaxially arranged fuel pressure atomizer. The cross–flow is realized by utilizing a 20–nozzle FLOX®–based natural gas combustor. Measurements include visualization of the reaction zone and analysis of the exhaust gas emissions. By detecting the hydroxyl radical chemiluminescence (OH–CL) emissions, the position of the heat release zone within the combustion chamber is attained. Correspondingly, the flame height above burner and the flame length are calculated. The investigated design parameters include air preheat temperature up to 733 K, equivalence ratio, burner geometry, and thermal power. The work presented in this paper aims to deepen the understanding of the design parameter interactions involved within the single–nozzle liquid–FLOX®–based burners. The cross–flow is set at a constant operating point to take the influence of the circulating hot gases on the flame into account. Through variation of thermal power the effect of liquid fuel preparation, i.e., atomization, evaporation, and mixing on combustion properties and exhaust gas emissions are examined. Analyses of measurements of different burner configurations are shown. The results show that the burners with the medium diameter consistently performed remarkably at different flame temperatures and thermal powers. The lowest NO_x and CO emissions for the medium diameter burner lied between 5 – 7 ppm and 8 – 10 ppm, respectively. The collected data sets can be used for the validation of numerical simulations as well.*

Keywords: FLOX®, single nozzle burner, liquid fuel, micro gas turbine, hydroxyl radical chemiluminescence (OH*–CL), Capstone C30, emissions, operating range.

NOMENCLATURE

Latin Letters

D_x	[-]	Normalized burner orifice diameter
p	[bar]	Pressure
P_{th}	[kW]	Thermal power
v_{nozzle}	[m/s]	Nozzle jet velocity

Greek Letters

λ	[-]	Air equivalence ratio

Acronyms

3D	3 Dimensional
ATM	Atmospheric
C30	Capstone C30 Micro Gas Turbine
CO	Carbon Monoxide
CO_2	Carbon Dioxide
CCD	Charge Coupled Device
CFD	Computational Fluid Dynamics
DLR	Deutsches Zentrum für Luft- und Raumfahrt (German Aerospace Center)
DMLS	Direct Metal Laser Sintering

FL	Flame Length
FLOX	Flameless Oxidation
HAB	Height Above Burner
LBO	Lean Blow-Off
LHV	Lower Heating Value
MILD	Moderate or Intense Low-oxygen Dilution
MGT	Micro Gas Turbine
NO_x	Nitrogen Oxides (NO + NO_2)
OH*–CL	Hydroxyl Radical Chemiluminescence
ORZ	Outer Recirculation Zone
PDI	Phase Doppler Interferometer
REX	Range Extender
TC	Thermocouple
UHC	Unburned Hydrocarbons

1. INTRODUCTION

The term FLOX® [1] is an acronym for "flameless oxidation". The term describes a type of a flame with very low carbon monoxide CO and nitrogen oxide NOx emissions [2]. Recently developed FLOX®–based burners offer promising potentials for fuel flexibility [3].

The working principle of the single–nozzle liquid fuel FLOX®–based burner is based on high momentum air–fuel mixture axially entering the combustion chamber. The high velocity turbulent jet entrains the combustion chamber gas that leads to strong gas backstream around the burner's axis. These recirculation zones cause a return of hot exhaust gas to the root of the jet, where it mixes with the entering fresh gas, which in return supports the flame stabilization and leads to eliminating local regions of high temperature within the reaction zone [4]. Ideally, through mixing the liquid fuel and oxidizer (air) upstream of the reaction zone, a homogenous combustible mixture can be formed that if operated at high air equivalence ratios, a reduction in NO_x emissions can be achieved [5].

Due to high exit velocity of the fresh gas, the effect of the ignition delay overrides the flame velocity as a flame stabilization factor, especially in lean conditions. As a result, the reaction rate of the fresh gas is reduced that allows for an improved mixing of air and fuel within the combustion chamber. Consequently, a stretched reaction zone can occur that in rare cases leads to combustion processes with scarce optical visibility of the flame formation [6]. A further detailed experimental tests conducted by Severin et al. [4] studying the recirculation stabilized jet flames showed a strong turbulent flame and the occurrence of self-ignition at the flame root. His experiments showed that since the trend of the flame's lift-off height and the ignition delay insufficiently correlate, the combustion is not exclusively based on ignition delay but is supported by it. Furthermore, Severin et al. [4] concluded that the continuous flame wrap-up is primarily responsible for the flame stabilization.

A C30 Capstone micro gas turbine is reutilized by Kislat et al. [7] as an electric vehicle range extender REX, where major components of the MGT undergo redesigning procedures for achieving higher overall efficiencies. For this purpose, the current study's burner system is designed and tested so that it can improve the MGT's fuel flexibility; reduce size and weight, while reducing the toxic emissions. In addition, the original air–blast spray technique of the MGT is replaced by a simplex pressure atomizer to maximize the MGT efficiency. A further study on the C30 MGT using liquid fuel as an electric vehicle range extender is conducted by Chen [8] showed ultra–low NO_x emissions through an optimization of the combustion system (injector and control) over a wide operational range of 50% to 100% .

In order to achieve the required targets of reducing CO and NO_x emissions and realization of fuel flexibility that enables burning a wide range of fossil and bio fuels, the potentials of three configurations of single–nozzle liquid fuel FLOX®–based burners are investigated and evaluated.

Some research studies have previously been conducted on FLOX®–based burners. In particular, experiments conducted by Gounder, et al. [9] studied the spray characteristics in a new liquid fuel 8–nozzle FLOX®–based combustor for MGT applications. Gounder's investigation showed a stable flame at high jet velocity and lambda-based global air equivalence ratio of v_{nozzle} = 120 m/s and λ = 1.45, respectively. The work conducted by [9] provided comprehensive data for CFD simulations for better understanding the evaporation process taking place in the flames of the liquid FLOX®–based burner.

Principally, the liquid fuel FLOX®–based burners carry a set of additional challenges when compared to a gas burner, which need to be addressed. The first challenge is the liquid fuel preparation, which is mainly in form of atomization and its subsequent vaporization. An alternative method of liquid fuel preparation is addressed by Gokulakrishnan et al. [10], where a premixed and prevaporized combustion system is utilized to characterize the effects of gaseous fuel and prevaporized liquid fuels on the exhaust gas emissions of a swirl based combustor system .The second challenge is related to the creation of a combustible air–fuel mixture that can considerably influence the combustion efficiency and emitted toxic gases. Extensive research on FLOX® (a subclass of Moderate or Intense Low-oxygen Dilution MILD) combustion has been conducted by Weber et al. and Lee et al. [11,12] on liquid as well as gaseous fuels that showed great potentials in lowering CO and NO_x emissions. The MILD combustion is defined by Cavaliere & Joannon [13] as "*a combustion process where the inlet temperature of the reactant mixture is higher than mixture self-ignition temperature whereas the maximum allowable temperature increases with respect to inlet temperature during combustion is lower than mixture self-ignition temperature (in Kelvin)"*. In this manner, the combustion process occurs in excessively sub-stoichiometric conditions for entrainment of large amount of recirculating flue gases into the fuel jets before ignition [12]. All these conducted works surrounding FLOX®–based combustion process is essential since gaining knowledge about governing parameter relations affects the flame operating range and geometrical properties, the MGT operational strategy, which in return determine the MGT's overall efficiency, emissions, its combustion chamber length, and life span.

The original fuel atomization technique of the C30 MGT is based on air–blast fuel atomization principle that is replaced by simplex pressure atomizers, in order to increase the efficiency of the MGT. This is achieved through discarding the expensive and heavy air compressor needed for the air–blast atomizers. Krishna [14] conducted tests on the original C30 MGT's atomizers using biodiesel blends to analyze the spray behavior of the atomizer at a variety of fuel properties. In previous works, conducted on characterizing several off–the–shelf simplex pressure atomizers, it was discovered that a fuel atomizer manufactured by the company DIVA Sprühtechnik performed superiorly when compared to fuel nozzles of different manufacturers [15,16]. The current work essentially acts as a supplementary study to furthermore point out the influence of burner diameter, air equivalence ratio, and thermal power variation rather than the mere impact of the atomization quality of different atomizers and the distance between atomizer and burner head. Bolszo et al. [17] investigated the impact of biodiesel on fuel preparation and emissions for a liquid fuel fired MGT. The results showed that the evaporation time of the liquid fuel increases with the decrease of the atomization quality. In his study, due to higher viscosity of the biodiesel compared to fossil–based diesel, larger droplets were produced by the atomizers, which consequently lead to higher NO_x and CO emissions.

In a related work conducted by Wei et al. [18] the effects of operating parameters, i.e. the velocity of air and fuel injection, the preheated air temperature, etc., on NO_x emission and parameters optimization to reduce NO_x emission for high-temperature air combustion using computational fluid dynamics were compared with experimental data. The results of the parameter characterization showed that among other parameters, the air velocity had a significant influence on NO_x formation, where by increasing and decreasing the air velocity the NO_x levels were reduced and raised, respectively.

A further study investigating the effect of liquid fuel preparation, i.e. atomization and evaporation, on emissions from an industrial gas turbine engine has been conducted by Nakamura et al. [19]. In this study, the performance of a fuel injector in preparing the air–fuel mixture for combustion was investigated in the laboratory at actual engine conditions using PDI and flow visualization. Nakamura's study concluded that superior atomization and evaporation of an injector does not necessarily translate into improved emissions. In other words, while atomization and evaporation play a vital role in the fuel preparation, they are however, of secondary importance to the air–fuel mixing before and in early stages of the reaction, as far as the NO_x emissions are concerned.

2. EXPERIMENTAL SETUP

In the current research, the experiments are carried out on an atmospheric test rig that was newly designed for generic tests on various burner concepts for MGT applications. The experimental test rig comprises of two combustor systems, liquid fuel preparation system, natural gas supply system, and two high temperature combustion air supply systems. The test rig's arrangement is based on the tangentially arranged three-burner configuration that is adopted from the original C30 MGT combustor system (see section 2.2). Different process parameters are kept constant according to the MGT condition for enabling an extensive experimental analysis that provides realistic database for further development of the MGT burner.

2.1 Liquid Fuel Burner Configurations

Preliminary results from a previous study of numerical simulations of one of the tested burners are shown in Fig. 1a and 1b, which depict longitudinal sectional views through the burner axis to demonstrate the FLOX® principle at 3.5 bars and 1 bar, respectively. Since the tests are conducted at atmospheric pressure condition, the burners are geometrically scaled, in order to attain the burner exit velocity at the MGT pressure condition (3.5 bars). Equation 1 shows the geometrical scaling factor using Mach number similarity calculated for the current study. Using the ideal gas equation for both atmospheric as well as MGT conditions, the only varying parameters are the pressure p and the burner discharge orifice diameter D. Other parameters which remain constant for both of the atmospheric and MGT test are: the air mass flow rate, the jet velocity (residence time), and the air preheat temperature. Therefore, for p_{MGT} = 3.5 bars the multiplication factor for the MGT burner diameter is $\sqrt{3.5}$.

$$D_{ATM} = D_{MGT}\sqrt{\frac{p_{MGT}}{p_{ATM}}} \quad (1)$$

Unlike the common technique of scaling the thermal power of the burners at atmospheric condition, for the current work, it is emphasized that the thermal power should not be scaled due to the altering behavior of the pressure atomizers incorporated within the current burner system. For the sake of keeping the main operating parameters constant, such as air mass flow rate, air preheat temperature, the thermal power, and the burner discharge velocity, it is opted to scale the burner discharge radius for the atmospheric tests.

As seen in Fig. 1a and 1b, the profound outer recirculation zone ORZ can be recognized through the streamlines that represent the flow at 3.5 bars and 1 bar pressures, respectively. High velocities up to 120 m/s can be seen in the CFD simulation that account for the need of a unique flame stabilization technique. The occurring stagnation points (axial velocity v = 0 m/s) ensure a stable flame despite the local high velocities.

The coaxial burners with the three discharge diameters allow for high momentum jet flows that lead to creation of intense mixing of hot and combustible gases, which reduce peak

temperatures in the downstream of the flame [20]. Thus, thermal NO emissions can be suppressed.

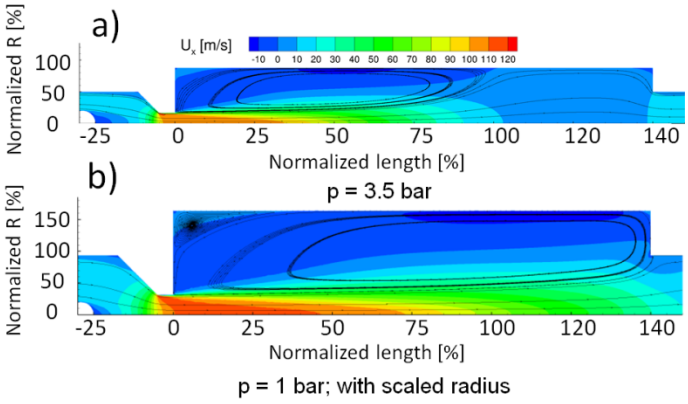

FIGURE 1: RESULTS FROM A NUMERICAL SIMULATION SHOWING AXIAL VELOCITY OF D_2 BURNER AT FULL LOAD; A) CFD SIMULATION AT 3.5 BAR MGT PRESSURE, B) SCALED BURNER AT 1 BAR FOR ATMOSPHERIC TESTS

The experimental investigation of the FLOX®–based burners is conducted at the test facilities of the DLR Institute of Combustion Technology. Through the atmospheric experiments a better understanding of jet stabilized liquid fuel flames can be attained that plays an important role in designing and developing novel MGT FLOX®–based burners.

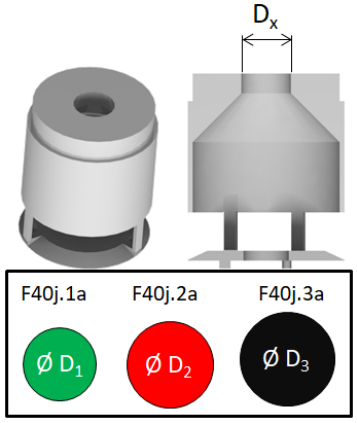

FIGURE 2: OVERVIEW OF THE LIQUID FUEL SINGLE–NOZZLE FLOX®–BASED BURNERS' GEOMETRY IN ISOMETRIC (UPPER LEFT) AND SECTIONAL VIEW (UPPER RIGHT)

The investigated burners shown in Fig. 2 are made of Inconel and are manufactured by 3D printing technology (direct metal laser sintering DMLS) that are post–processed to reach the required nozzle diameters. The burners are vertically mounted and are tested in three discharge orifice diameter variations: F40j.1a (D_1), F40j.2a (D_2), and F40j.3a (D_3). For an easier traceability of the burners, the designation of D_1, D_2, and D_3 will be used throughout this work. It is worth mentioning that the burners are designed in a way that the diameter of the D_2 is varied by ±10%. In other words, $D_1 = 0.9 \times D_2$ and $D_3 = 1.1 \times D_2$. As seen in Fig. 3, preheated air enters the burner after being redirected via a diffusor that emulates the same diversion of the air occurring within the MGT burner. In addition, this causes the air to enter the burner with less turbulence. As depicted in Fig. 3, the fuel nozzle is placed below the burner exit nozzle ejecting liquid fuel (blue triangle) axially downstream the air flow (orange streamline). The liquid fuel atomizer is located 2 x D_2 below the burner head to minimize spray burner–wall interaction. Finally, the fuel and air are partially premixed and are directed through a conically shaped nozzle to further increase their velocity while entering the flame tube for initial ignition and then chemical reaction. The quartz glass flame tube that connects the burner to the combustion chamber is mounted above the burner and has an inner diameter of 3.2 x D_2 and an axial length of 6.3 x D_2 (burner front plate to entrance of the combustion chamber). The flame tube provides optical access from all four sides. This allows for multi–direction optical measurement. The combustion chamber is mounted on top of the flame tube that consists of four quartz glass walls (see Fig. 5). The liquid fuel used for this set of experiments is JetA–1. For optimal preheated air temperature measurement, four N-type thermocouples (TC) are installed within the plenum to monitor and record the electrically preheated air temperature (see Fig. 3).

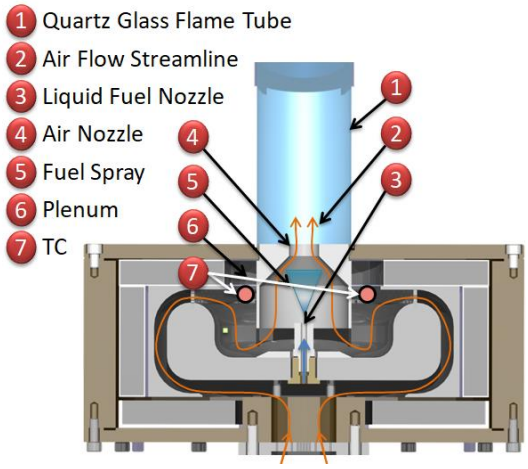

FIGURE 3: SECTIONAL VIEW OF THE LIQUID FUEL TEST RIG DETAILING THE MAIN COMPONENTS OF THE EXPERIMENT

The liquid fuel atomizer DIVA is depicted in Fig. 4a along with its casing and orifice diameters of 10 and 0.2 mm, respectively. The data provided by the manufacturer of the nozzle include the designed spray angle of 80° at a pressure drop of 3 bars and a capacity of 0.73 g/s of water as fluid medium (see Fig. 4b). For the current experiments, a fuel mass flow rate of 0.88 g/s is needed for 100% thermal power of a single burner. This flow rate required a fuel pressure drop of 10 bars, which is due to a higher mass flow rate extended the spray angle to roughly 92° (see Fig. 4c). It is worth mentioning that due to differences in thermal properties of the fuel used in this study and water used as test medium, the spray angle of the nozzle can slightly vary.

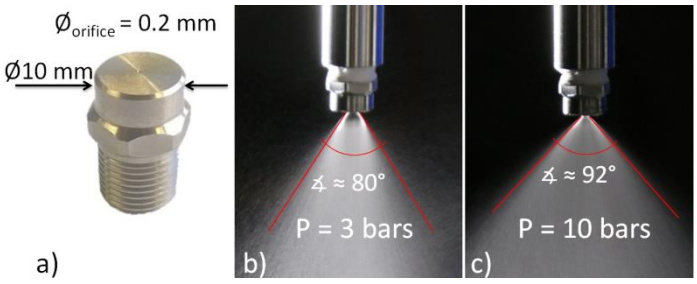

FIGURE 4: OVERVIEW OF THE LIQUID FUEL ATOMIZER DIVA; A) GEOMETRICAL PROPERTIES OF THE DIVA NOZZLE [15], MIE SCATTERING IMAGES SHOWING SPRAY ANGLE OF THE NOZZLE AT B) 3 BARS AND C) 10 BARS PRESSURE DROP USING WATER AS FLUID MEDIUM

2.2 Hot Gas Generator

As mentioned before, the FLOX®–based burner is intended to be used in the C30 MGT, which incorporates three tangentially aligned burners around its annular combustion chamber (see Fig. 5a). Basically, the current experiment considers the entire C30 MGT combustion chamber, while only one of the three burners of the C30 is actually tested and the rest of the two burners are emulated in form of a hot cross–flow that joins the flame of the experimented single nozzle liquid fuel burner in the optical combustion chamber (see Fig. 5b). The hot cross–flow gas is generated by a separately operated 20–nozzle FLOX®–based natural gas burner [21] as shown in Fig. 6. In this manner, the effect of the hot cross–flow on the liquid fuel flame can be more explicitly characterized. However, the comprehensive investigation of the cross–flow will be conducted in a separate set of experiments using Design of Experiments as a modern technique in conducting and evaluating experiment results.

Although there are major similarities between the actual C30 MGT 3-burner configuration (Fig. 5a and 5c) and the atmospheric test rig (Fig. 5b and 5d), there are also a few distinct differences. On the one hand, the similarities include: a) the actual liquid fuel burner air and fuel flow rates, i.e. the MGT based thermal power and jet air velocity without scaling, b) the flame tube length, c) the angle in which the hot gases enter the combustion chamber enabled by utilizing a flow ramp (Fig. 5b), the offset between the burner and the combustion chamber (Fig. 5c and 5d). On the other hand, the differences include: a) lack of recirculation of gases that could dwell within the MGT annular combustion chamber longer than the atmospheric optical combustion chamber, b) the operating combustion chamber pressure, c) the neglected variation of the hot gas generator operating parameters, i.e. adiabatic temperature, hot gases velocity, and thermal power, and d) the exhaust gas emissions difference of the hot gas cross–flow running via a natural gas burner rather than two liquid fuel burners.

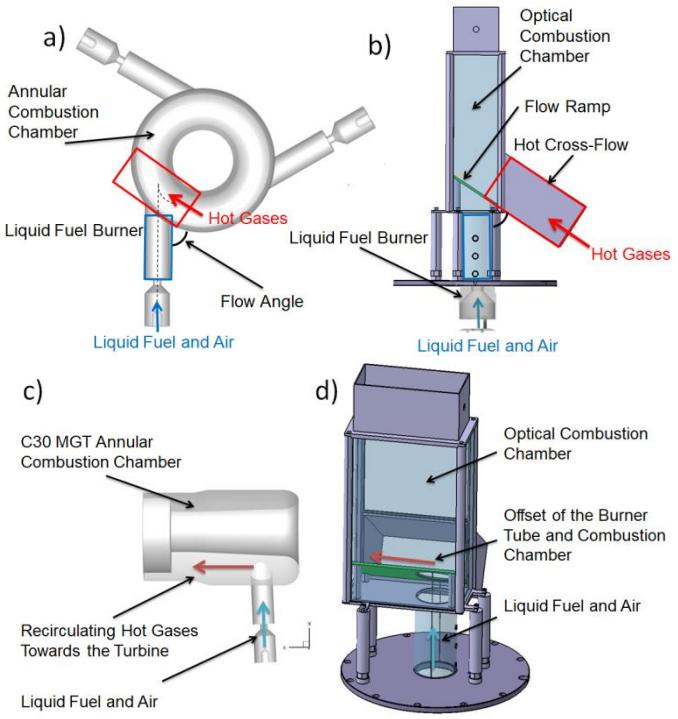

FIGURE 5: A) SECTIONAL TOPVIEW OF THE C30 MGT COMBUSTION CHAMBER AND BURNERS, B) THE EQUIVALENT EXTRACTION OF THE MAJOR GAS FLOWS FROM THE MGT FOR THE ATMOSPHERIC TESTS, C) SECTIONAL SIDEVIEW OF THE C30 MGT COMBUSTION CHAMBER, D) SIDEVIEW OF THE ATMOSPHERIC LIQUID FUEL TEST RIG

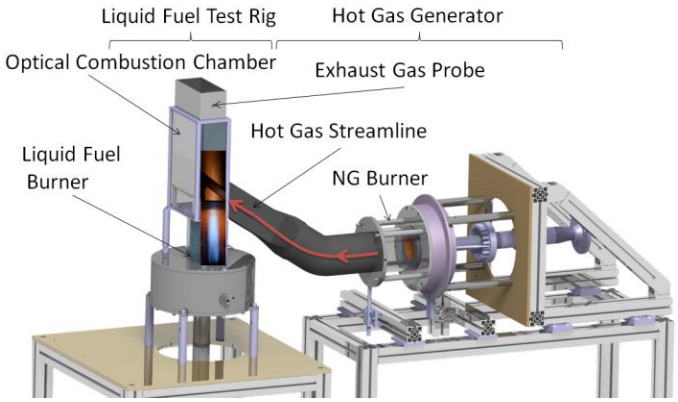

FIGURE 6: ATMOSPHERIC EXPERIMENTAL SETUP: REPRESENTATION OF BOTH OF THE LIQUID FUEL AS WELL AS THE NATURAL GAS BURNERS

It is worth mentioning that for the current tests, the hot gas generator is set to a constant set point throughout all of the experimental campaign, since merely the liquid single nozzle FLOX®–based burners are target of the investigation and not its flame's interaction with the hot cross–flow. The analyzed emissions are based on the overall exhaust gases generated by the liquid fuel as well the hot cross–flow. Since the emissions of

the cross–flow are either higher or lower than the emissions of the liquid fuel burner depending on the operating conditions, thus a subtraction cannot be made. By operating the cross–flow burner at a steady operating point, its influence on the emissions of the liquid fuel burner will be equally propagated through all of the analyzed flames.

3. MEASUREMENT TECHNIQUES

For the current study, basic combustion diagnostic techniques are used in order to characterize the FLOX®–based liquid fuel burners. OH* chemiluminescence imaging is used to detect the shape and position of the flame zone for each run point. The flame length FL as well as the height above burner HAB of each flame are then calculated from the averaged OH* chemiluminescence images. A detailed overview on how these data are calculated can be found a previous work of Bower et al. [22]. The concentrations of major exhaust gases are measured and recorded for burner evaluation purposes. The exhaust gas emissions are extracted from the combustion chamber downstream of the liquid fuel flame, where a probe is positioned at the top of the rig, after both of the hot cross–flow gas and the flue gas of the liquid fuel burner are joined (see Fig. 5).

3.1 OH* Chemiluminescence Imaging

Capturing the OH* chemiluminescence of the flame is a commonly used technique of collecting information about the size and position of the heat release zone, due to the short lifetime of OH* that is produced within the reaction zone [23]. The OH* chemiluminescence signal intensity depends on the concentration of the electronically excited hydroxyl radicals that are mainly formed during the chemical reaction $CH+O_2 \rightleftharpoons CO+OH^*$ [24].

In this study the OH* chemiluminescence emissions are detected utilizing a LaVision High Speed Star charge coupled device (CCD) camera, which is coupled with a High Speed Intensified Relay Optics intensifier, a CERCO 100 mm F/2.8 UV lens and a UV interference filter (312 ± 15 nm). The signal is recorded at a constant gate time of 50 µs. For all measurements, 500 single instantaneous images are taken at a repetition rate of 1000 Hz. The images are subsequently processed by LaVision DaVis software in combination with an in–house software.

As depicted in Fig. 7, the OH* chemiluminescence field of view is axially centered on the liquid fuel burner. The entire reaction zone of the liquid fuel flame is captured by the camera, which is located perpendicularly 3000 mm distanced from the liquid fuel burner. Not only can the field of view of the camera capture the entire liquid fuel flame but also the entrance of the hot cross–flow channel into the combustion chamber. Hence, the influence of the hot gases on the flame can be visually recorded.

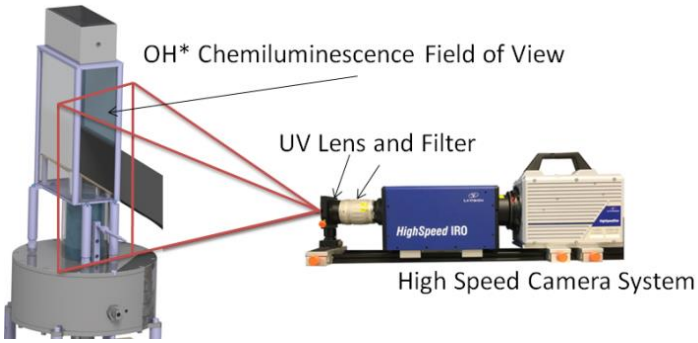

FIGURE 7: OH* CHEMILUMINESCENCE EMISSIONS CAPTURING SETUP CONSISTING OF ICCD CAMERA, UV OPTICAL LENS, AND INTERFERENCE FILTER

3.2 Emissions Measurements

During each operating point, exhaust gas measurements are conducted using an ABB process gas analyzer (Advanced Optima Process Gas Analyzer AO2000) and are subsequently evaluated. The flue gas samples are taken at the top of the liquid fuel combustion chamber through a specially designed air cooled probe, which cools the gas down to 180 °C, in order to preserve the chemical composition of the flue gas sample. The gas analyzer is able to detect water vapor H_2O (Vaisala–HMT330), carbon dioxide CO_2 (ABB Uras26), and oxygen O_2 (ABB Magnos206) content, as well as carbon monoxide CO (ABB Uras26), unburnt hydrocarbons UHC (ABB MultiFID14 NMHC), and nitrogen oxide (NO_x: sum of the NO and NO_2) (ABB Limas11) concentrations. The measured water vapor content is then used to calculate the results in dry conditions. In addition, the absolute emission concentrations are normalized to 15% O_2 content. The measured data are recorded at a frequency of 1 Hz for a minimum of 3 minutes of a stable operating condition. The standard deviation of the calculated data is so small that is not depicted in the diagrams. An overview of the utilized ABB gas analyzer is shown in Table 1.

Table 1. ABB PROCESS GAS ANALYZER ACCURACIES AT DIFFERENT RANGES.

Species	CO (ppm)	UHC (ppm)	NO_x (ppm)	O_2 (Vol.–%)	CO_2 (Vol.–%)
Range 1	0–10	0–19	0–10	0–5	0–5
Accuracy	0.1	0.37	0.1	0.025	0.05
Range 2	0–100	0–187	0–20	0–15	0–20
Accuracy	1	3.73	0.2	0.075	0.2
Range 3	0–200	0–3733	0–50	0–25	
Accuracy	2	74.7	0.5	0.0125	
Range 4	0–500	0–9322	0–200	0–100	
Accuracy	5	186.6	2.0	0.5	

As shown in Fig. 8, the single point exhaust gas probe [28] is composed of an integrated double tube body where exhaust gas is sucked into the probe, while the gas is cooled to ca. 180 °C prior to entering the heated pipe that leads the gas to the ABB gas analyzer. Consequently, the gas and probe surface interaction

can be prevented by rapidly lowering the gas temperature to a point where water vapor condensation does not occur.

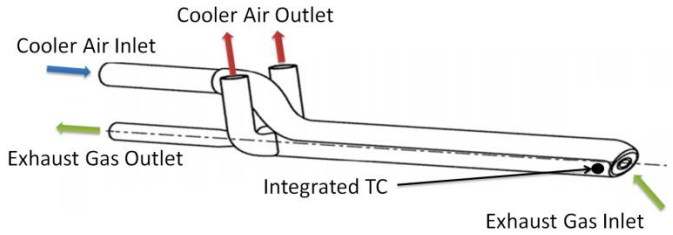

FIGURE 8: DESCRIPTION OF THE INCORPORATED EXHAUST GAS PROBE [28]

4. OPERATING CONDITIONS

The D_2 single nozzle FLOX®–based burner was initially designed on the basis of numerical simulations for an operating point of pressure p = 1 bar, air preheat temperature T = 738 K, and air equivalence ratio of $\lambda = 1.8$ using Jet A–1 as the liquid fuel (lower heating value LHV = 43.195 kJ/$g_{Jet\ A-1}$). The adiabatic flame temperature calculated for this operating point amounts to T_{ad} =1934 K.

Air momentum variation of the single nozzle FLOX® – based burners D_1, D_2, and D_3 is realized through constructing a test matrix, which runs air equivalence ratio sweeps, i.e. air mass flow rate variation at constant thermal power. In this study, the characterization of the burner in the atmospheric test rig is conducted at various operating conditions. For realization of various adiabatic temperatures a sweep of air equivalence ratios are run. In order to inspect the influence of different thermal power levels, liquid fuel flow rate is varied. Meanwhile, the air preheat temperature is kept at a constant level, so that it corresponds to the actual condition of the C30 MGT at 738 K. The fuel atomizer is not varied, for a better comparability between the results. The characterization of the fuel atomizer was conducted by [15] in a previous study. Based on his experiments, a series of off-the-shelf atomizers from different manufacturers at different nozzle –burner distances were tested and characterized according to their flame geometrical properties using OH* chemiluminescence, i.e. flame length and height above burner. An overview of the operating conditions is given in the Tab. 2.

Table 2. OVERVIEW OF THE CONDUCTED STUDY OPERATING CONDITIONS. RANGE OR MAXIMAL VALUES OF AIR NOZZLE DIAMTER $Ø_{NOZZLE}$, PRESSURE P, AIR PREHEAT TEMPERATURE T_{PRE}, AIR EQUIVALENCE RATIO λ, AND THERMAL POWER $P_{THERMAL}$ FOR ALL THREE SINGLE NOZZLE FLOX®–BASED BURNERS

Parameter	Unit	Range
$Ø_{Nozzle}$	[%]	90, 100, 110
p	[atm]	1
T_{pre}	[K]	738
λ	[–]	1.1 – 1.66
$P_{thermal}$	[kW]	28 – 49.4

The 20–nozzle natural gas FLOX®–based burner is run at a constant operating point throughout the entire experiments at 673 K preheated combustion air, 50 kW thermal power, and air equivalence ratio 2.4. Variation of the hot gas generator is purposely neglected, since the current tests address only the influence of the burners' discharge orifice diameter on the flame stability and geometry.

5. RESULTS AND DISCUSSION

For a comprehensive analysis of the burners, it is recommended not only to characterize the flames according to their exhaust gas emissions, but also the flame–specific geometrical properties have to be taken into consideration. In this part, main emission graphs for exhaust analysis of different operating points of the liquid fuel burner will be examined.

5.1 Investigation of Optimum Emission Operation

In order to further analyze the influence of various part loads of the MGT burners on the exhaust gas emissions, the concentrations of the NO_x and CO are shown in the following graphs. For better representation purposes, the concentrations of the emissions are normalized to 15 Vol–% O_2 at dry conditions. Three major experimental parameters are varied that have considerable influence on the flame stability and exhaust gas emissions. The burner discharge orifice diameter, air equivalence ratio, and thermal power are varied to influence the jet velocity, the flame temperature, and the released heat rate, respectively.

Figure 9a shows the respective NO_x and CO concentrations for the variation of air equivalent ratios, while all three single nozzle FLOX®–based burners are operated at a thermal power of 28 kW, atmospheric pressure, and preheated air temperature of 738 K. The effect of the air equivalence ratio variation is clearly visible: NO_x is reduced for decreasing flame temperatures (increasing air equivalence ratio). The same trend is applicable to the CO concentrations for all three burners. With regard to both NO_x and CO concentrations, the D_2 with the medium discharge orifice (curve with round symbol) shows the best performance. This is due to enhanced interaction of the smaller unstable vortices in the shear layer between the D_2 burner recirculation, hot exhaust gas, and fresh gas. As a result of this, a more significant mixing of the hot gases within the reaction zone is achieved that leads to decreased thermal NO_x formation. The CO concentrations of all the three burners fall slightly less significantly than NO_x concentration.

As shown in Fig. 9a, the emissions of the burner D_1 with the smallest discharge orifice behave moderately in comparison to the rest of the two burners. Its NO_x and CO concentrations are greater the D_2 but less that the burner D_3. A feature of the Fig. 9a is that, the burner D_1 shows a relatively reduced operation range, as its flame blow–off (LBO) occurs at λ = 1.57, whereas the rest two burners continue a stable operation. This premature LBO limit is due to higher jet velocities caused by the smaller diameter of the D_1 burner at high air equivalence ratios, which leads to lower reactivity and lower flame temperature.

Figure 9b depicts another series of NO_x and CO concentrations for various air equivalence ratios while operating the burners at a thermal power of 38 kW (increased fuel mass flow rate). Analog to Fig 9a, a similar influence of the burner discharge diameter can be found in this part load regarding the emission concentrations and flame stability.

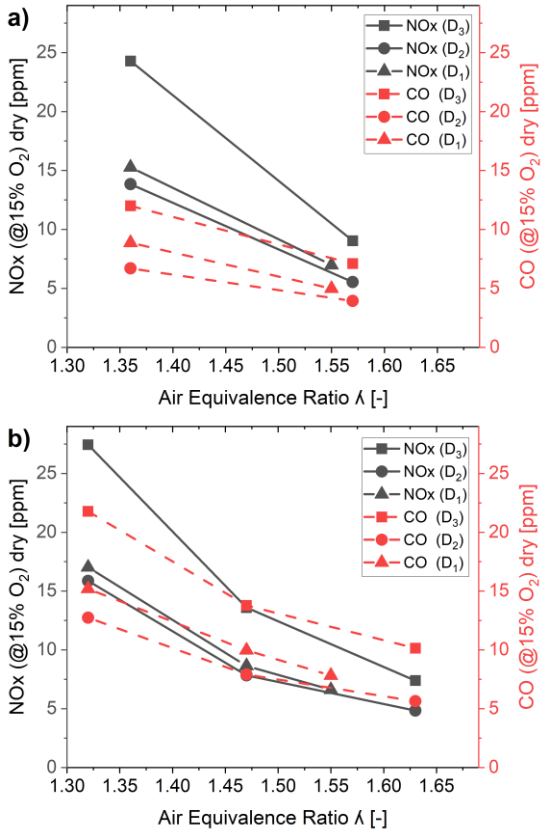

FIGURE 9: EXHAUST GAS CONCENTRATIONS (LEFT AXIS) NO_x, (RIGHT AXIS) CO FOR A VARIATION OF AIR EQUIVALENCE RATIO λ OF ALL THREE LIQUID FUEL FLOX®–BASED BURNER ORIFICE DIAMETERS: D_1, D_2, AND D_3; A) EMISSIONS AT 28 KW; B) EMISSIONS AT 38 KW THERMAL POWER

The dominant difference between both of the loads lies in the extended LBO limit that is observable in Fig 9b. Its cause can be rooted back to the improved atomization quality of the fuel nozzle at 38 kW load and higher jet velocities that improve droplet dispersion and evaporation by strong shear forces. For each operating point, the LBO limits are tested three consecutive times for gaining a higher statistical power. The D_3 burner shows anew the highest values of NO_x and CO concentrations at rich stages and decreasing concentrations towards the lean flames. The same principles of intense formation of thermal NO_x at higher flame temperatures can be applied to this load as well. The operational range of the D_1 burner has not changed during this series of experiments, for the reason that the jet velocity produced by the burner is considerably higher than the rest of the burners at this load. For instance, at $\lambda = 1.63$ the burners' discharge air velocity amounts to $v_{nozzle-D1} = 113.5$ m/s, $v_{nozzle-D2} = 92$ m/s, and $v_{nozzle-D3} = 76$ m/s.

Variation of the thermal power in liquid fuel combustion processes using a pressure fuel atomizer can make a noticeable change in terms of flame stability and emissions behavior, the spray characteristics vastly change when fuel mass flow rate is varied. The atomization of the liquid fuel degrades or improves while reducing or increasing the fuel pressure loss of the fuel nozzle, respectively [15].

Regardless of the thermal power in which the burner is operated, the trend of falling NO_x and CO concentrations with the rising air equivalence ratio is maintained (see Fig. 10a and 10b). The typical CO U–shaped trend with a distinct minimum, where the left branch follow the equilibrium conditions and the right branch follow the non–equilibrium conditions [5, 21, 25] cannot be observed in this series of experiments.

This unconventional behavior of the CO emission can be observed in previous FLOX®-based burner studies conducted with gaseous fuels [20] as well as liquid fuels [26, 27]. The reason behind the behavior of CO is the limited operation range of the burners. In a previous study [15], the D_2 burner was studied with similar experimental setup except for the flame tube geometry. The recorded LBO limit of 2.4 [15] was observed compared to the current LBO of the D_2 burner of 1.6. The mere difference of the experimental setup was the flame tube diameter of the burner, which measured 16 % larger than the current 3.2 x D_2 inner diameter. These key differences in the operating range and the geometry variation carry valuable information on this specific CO trend. Therefore, a limited operability of the burner and a "premature LBO" could play a role in the CO behavior. There are two general explanations on why the FLOX®-based liquid fuel burner flame blew off. Firstly, as the flame lifts up at higher air equivalent ratio, the recirculation of the hot exhaust gas that re-ignites the flame at its root is not hot enough to maintain the continuous re-ignition. This occurs when the recirculated gas, due to the lifted flame, is mainly dominated by the fresh gas, which has a relatively lower temperature. Secondly, a deteriorated air-fuel mixture that exits the burner at high velocities, limiting the mixture's time until sufficient evaporation occurs at the flame root, where rapid re-ignition takes place.

The evaluated emissions data indicate that regardless of the thermal power, the D_2 burner shows the most optimum NO_x and CO concentrations at all of the tested flame temperature ranges. It is therefore reasonable to further investigate the toxic exhaust gas emitted by the burner at various MGT corresponding part loads, as it demonstrates high potentials in terms of producing the least CO and NO_x emissions.

In another series of investigations with the D_2 liquid fuel FLOX®–based burner, five part loads of the C30 MGT are explicitly experimented at various air equivalence ratios (Fig. 10a and 10b). Running these experimental points allows a deeper characterization of the burner as to where its operational range lies. In addition, valuable information about the MGT's exhaust gas emissions at full load 100% as well as lower part loads (88%, 73%, 60%, and 45% load) can be obtained (see Fig. 10a and 10b).

As for the NO_x (Fig. 10a) concentrations in all thermal power ranges, a falling trend can be observed when increasing λ, where NO_x changes very minimally at different thermal powers at constant air equivalent ratios. A notable feature of this graph is the nearly linear NO_x behavior of P_{th}= 17 kW. It is clear that by decreasing the flame temperature, NO_x concentrations are decreased for all thermal powers P_{th}: 38 kW, 33kW, 28 kW, 23 kW, and 17 kW. For a constant air equivalence ratio, λ = 1.5, the least NO_x gas are emitted while the burner operates at the 100% load (38 kW for one burner) of C30 MGT and it increases when the load is decreased.

When decreasing the thermal power of a liquid fuel burner using pressure atomizers, there are two major phenomena that need to be considered. Firstly, degradation of atomization quality when fuel mass flow rate is reduced (decreasing thermal power) that leads to formation of larger fuel droplets, which in return induce local rich zones with too high temperatures. Secondly, for a constant air equivalence ratio, a decrease in thermal power reduces jet velocity that in part forms a less profound recirculation zone around the flame. This can cause a degraded mixing of hot gases due to weaker shear forces that can lead to more local rich zones within the reaction zone.

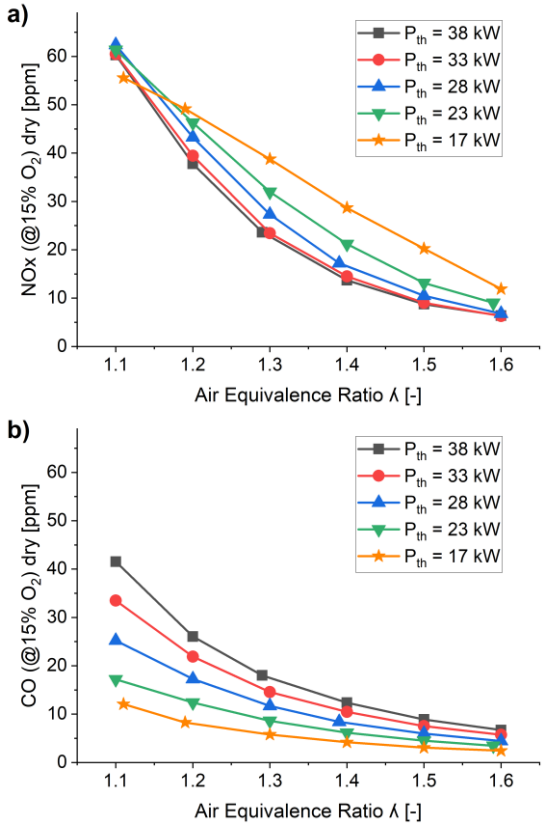

FIGURE 10: EXHAUST GAS CONCENTRATIONS VS. AIR EQUIVALENCE RATIO λ FOR A SERIES OF THERMAL POWERS P_{th} FOR D_2 LIQUID FUEL FLOX®–BASED BURNER; A) NO_x EMISSIONS; B) CO EMISSIONS

In an overall observation between the entire thermal power ranges the CO concentrations (Fig. 10b) show an increase by the increasing the thermal power, which is due to decreased residence time of the CO molecules that evade their oxidation into CO_2 [21]. The lowest CO concentrations are measured while running the D_2 burner at 17 kW thermal power (45% load for one burner of the C30 MGT). The reason behind this behavior is the relatively low jet velocity of the operating points at P_{th} = 17 kW, which in return enhances CO oxidation due to its longer residence time within the reaction zone. Here, the advantageous annular combustion chamber of the C30 MGT should be mentioned that allows to an extended residence time of the exhaust gases within the chamber. This way, the CO emissions can greatly be reduced.

There is a variety of methods that can improve the emissions quality of the MGT. Firstly, by utilizing an operation strategy that explicitly targets the atomizers maximum flow rates, i.e. a strategy is made to turn on and off one or two burners when another part load is to be operated. It is learned that the NO_x emission (see Fig. 10a) of a single burner is increased by decreasing the thermal power. This means the flames of the burners produced the least NO_x, when operated at higher fuel mass flow rates. As shown in Table 3, a unique solution to this behavior is to turn off one burner out of three while running at lower MGT part load, e.g. 73% part load or 84 kW (28 kW per burner). Instead of reducing the mass flow of each of the atomizers, it opted that by shutting down one atomizer, the rest of the two atomizers will operating at a higher fuel mass flow rate (42 kW each). A clear advantage of this in terms of NO_x emission improvement can be observed Fig.10a and 11a are compared. In Figure 10a, the blue curve (with triangle symbols) shows the case, when the MGT is run at 73% part load or 3 burners × 28 kW = 84 kW. In this case, at λ = 1.3 a NO_x concentration of 27.3 ppm is recorded. Utilizing the operation strategy shown in Table 3 allows this particular operating point to produce a concentration that is reduced to 21.7 ppm as presented in Fig. 11a (blue curve with triangle symbols at λ = 1.3). Table 3 lists various part loads of the MGT and the viable strategy chosen on how many burners should be operating at which part load. For instance, at part load 60% there should be only 2 burners operating to achieve an improved NO_x emission.

Table 3. C30 MGT OPERATION STRATEGY AT VARIOUS LOADS; *Op. = Operating

load [%]	100	88	73	60	45	30	17
Burners Op.*	3	2	2	2	1	1	1
P_{th} [kW]$_{Burner}$	38.3	50.5	42	35	52	35	20
P_{th} [kW]$_{MGT}$	115	101	84	70	52	35	20

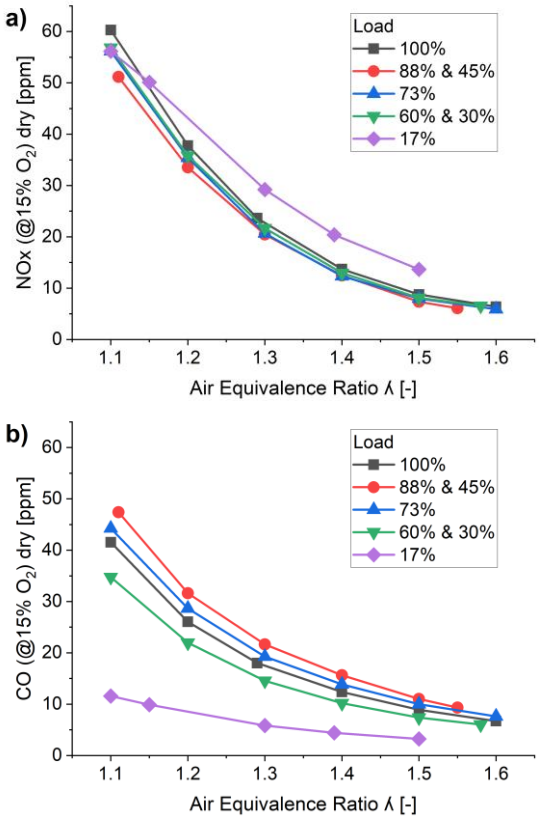

FIGURE 11: EXHAUST GAS CONCENTRATIONS VS. AIR EQUIVALENCE RATIO λ FOR THE MGT OPERATION STRATEGY USING D_2 BURNER; A) NO_x EMISSIONS; B) CO EMISSIONS

As shown in table 3, the 88% and 45 % part loads can result into similar emission concentrations, since at both of part loads; either two or one burner is operating with identical fuel mass flow rates, which results into similar emission concentrations. Comparable situation can occur while operating the MGT at 60% and 30 % operating point, where two and one burner are operating, respectively.

The CO concentrations depicted in Fig. 10b and 11b show similar trends and are not significantly different. An interesting highlight of the Fig. 9b is that the minimum part load of 17 % (purple curve with rhombus symbols), which its operation was only made possible when running with the chosen MGT operation strategy, as otherwise the fuel mass flow rate per burner would be too little that the injectors would choke through liquid fuel vaporization within the injectors.

5.2 Flame Characterization

The OH* chemiluminescence time averaged images of some of the operating points of the current study are depicted in Fig. 12a and 12b. It should be noted that the horizontal line on each flame is due to the blockage of the OH* emissions of the plate connecting the flame tube and the optical combustion chamber. The tangential line on the flames represents the blockage of the OH* emissions by the flow ramp metal plate redirecting the hot cross–flow gas into the combustion chamber. Here, the liquid fuel burner is located axially below each flame and the cross–flow is directed into the combustion chamber above the tangential line on the flame.

The top set of OH* chemiluminescence images (Fig. 12a) represent flames of the three burner discharge orifice diameters of D_1, D_2, and D_3 for three air equivalence ratios λ = 1.36, 1.47, and 1.63 at a thermal power of 38 kW. Considering the images of λ = 1.36 (12a left image-set), one can recognize the increased flame length of the burner with the smallest diameter D_1. Naturally, the jet velocity exiting this burner's orifice at the air equivalence ratio is the highest and this leads to lower flame reactivity rate that leads to a stretched flame. For the same λ, the flame of the burner with the largest diameter D_3 seems to have the largest of the reaction zones. For the current set of flames, the height above burner HAB of all three burners seem to be approximately constant (see also Fig. 13a).

For the flames in the upper image-set with the λ = 1.47, the HAB for the three burners are quite different, where the flame of the burner D_1 is lifted the highest among the rest of the flames. For the same thermal power and λ = 1.63, the flame of the burner D_1 had already reached its LBO limit, where the rest of the flames show furthermore stable flames, despite being quite lifted from the burner head (see Fig. 12a right image-set). Generally, the flame moves downstream with the decreasing flame temperature. As fuel flow rate is kept constant (constant thermal power), increasing the air equivalent ratio leads to an increase in air exit velocity, flame HAB, and the flame length. An increase in velocity also means increased turbulence and thus an increase in droplet evaporation rate [26].

As shown in Fig. 12b, by increasing the thermal power, i.e. increasing the ejected fuel mass flow rate from the atomizer, not only the quality of the fuel spray can be improved, but also rate of the heat released is elevated. Figure 12b shows flames for various air equivalence ratios at a constant thermal power of 43 kW. Similar to the previous image-set, experiments are run at different air equivalent ratios and burner discharge orifice diameter. The flames run at λ = 1.36 show the widest reaction zones with burner D_1 being slightly lifted higher than the rest two flames. This behavior is due to relatively higher jet velocity of the burner at the same operating conditions.

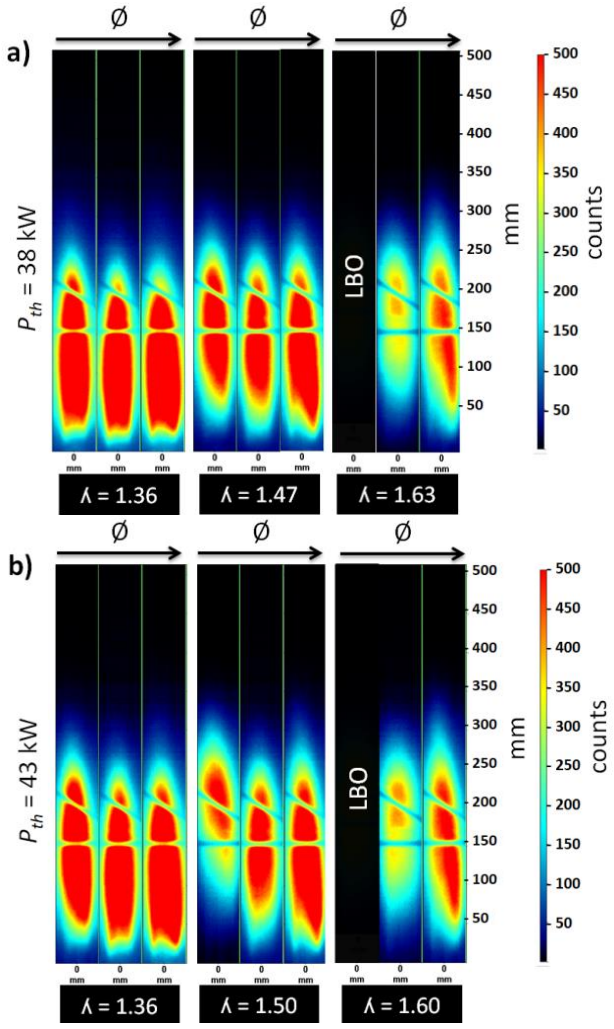

FIGURE 12: OH* CHEMILUMINESCENCE TIME AVERAGES IMAGES FOR VARIOUS BURNER DISCHARGE ORIFICE DIAMETERS, THERMAL POWERS P_{th}, AND AIR EQUIVALENCE RATIOS λ; A) FOR THERMAL POWER OF 38 KW, B) FOR THERMAL POWER OF 43 KW

The calculated correlation between the height above burner along with the flame length for a variation of air equivalence ratio and different burner diameters is displayed in Fig. 13a and 13b for thermal powers of 38 kW and 43 kW, respectively. As shown in Fig. 13a, the rising HAB with the increasing λ can be clearly seen. This is due to flame instabilities occurring at higher air equivalence ratios, caused by a lower reactivity rate. With increasing jet velocity and decreasing adiabatic temperature, the flame length increases, but at a lower rate compared to flame HAB. There are only two operating points recorded for the burner D_1, because it had already reached its LBO limit at λ = 1.5. It is assumed that the HAB variation of the burners largely depend on the conditions on which the liquid fuel burner is operated and the flame lengths of the burners vary very slightly due to the hot cross–flow gas entering the combustion chamber where the tip of the flames are. This, in return, acts like a limiting factor for the flame length that prevents the flames from large FL variation.

Figure 13b depicts the HAB and FL of the three burners at the thermal power of 43 kW. The trends of the curves are generally the same as in the Fig. 13a but with a few noticeable changes. The HAB of the burner D_1 varies from λ = 1.3 to 1.5 drastically, which was not seen in the case of P_{th} = 38 kW. This behavior derives back to the significantly increased jet velocity at this load that leads to reduced flame stability. Another highlight of the Fig. 13b is the falling flame length of D_1 from λ = 1.35 – 1.5. Here, the flame has nearly reached its LBO limit, which explains the instability of the flame due high jet velocities and lower reactivity rate.

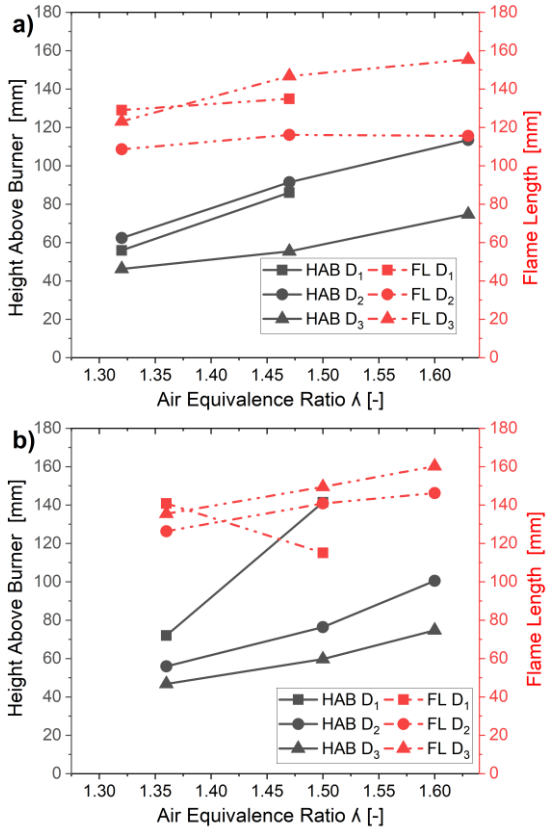

FIGURE 13: CALCULATED DATA FROM OH*–CL IMAGES; A) HEIGHT ABOVE BURNER AND FLAME LENGHT VS. λ FOR VARIOUS BURNER DIAMETERS AT P_{TH} = 38 KW, B) HEIGHT ABOVE BURNER AND FLAME HEIGHT VS. λ FOR VARIOUS BURNER DIAMETERS AT P_{TH} = 43 KW

Figure 14a and 14b represent explicitly the height above burner and flame lengths of the D_2 burner for air equivalence ratio and thermal power variation. The HAB depicted in Fig. 14a shows a rising trend when λ is increased and thermal power is decreased. The increasing instability of the flame is due to the lack of fuel richer flames, a lower flame temperature and heat radiation. On the contrary to the HAB the flame lengths decrease by decreasing the thermal power of the burner. As a vital priority in developing a burner for MGT application, the flame length plays an important role towards designing a compact combustor.

The flame lengths of 90 – 115 mm at P_{th} = 38 kW (100 % MGT load) seem to be acceptable, since the annular combustion chamber of the C30 allows for an extended room for longer flames.

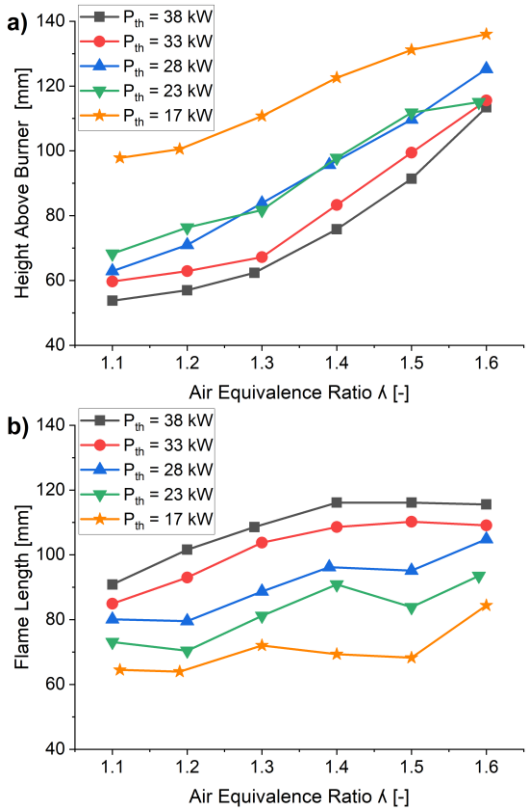

FIGURE 14: CALCULATED DATA FROM OH*–CL IMAGES OF THE D_2 BURNER ; A) HEIGHT ABOVE BURNER VS. λ FOR VARIOUS THERMAL POWERS, B) FLAME LENGTH VS. λ FOR VARIOUS THERMAL POWERS

6. SUMMARY & CONCLUSIONS

Three configurations of liquid burners based on FLOX® concept were tested at the Atmospheric Laboratory at DLR's Institute of Combustion Technology. Experiments on the burner discharge orifice diameter variation were considered the center point on the study. The conducted experiments revealed the full operability limit of all the three burner configurations using JetA-1 as the utilized liquid fuel at 1 atm pressure condition. The burners were operated stably in a range of air equivalence ratios λ (1.1 – 1.66) and thermal power P_{th} (19 – 49.4 kW). Two main measurement techniques were used to capture the data and characterize the burners: exhaust gas measurement and OH* chemiluminescence.

The exhaust gas analysis showed a minimum of 5 ppm of NO_x concentration at λ = 1.6 and P_{th} = 43 kW for the D_2 burner. This seems to be a result of good atomization quality of the fuel nozzle that lead to rapid evaporation rate of the liquid fuel within the reaction zone. Decent CO concentrations were measured while operating at higher jet velocities of the burners.

OH* chemiluminescence images have shown low height above burner and larger reaction zones at high flame temperatures and low jet velocities for all three burner configurations. By increasing the jet velocities of all the burners, there was a marginal change in the flame lengths as it seemed that the hot cross–flow gas had an influence on the maximum length of the flames.

The presented exhaust gas emissions of the studied burners can serve as validation data for numerical simulations as well as for further development of liquid fuel FLOX®–based burners. The future outlook for the further development of the burners should include reducing the flame length. For achieving this goal, a newly developed atomizers or even different methods of liquid fuel preparation such as pre-vaporization can be considered. In a previous study it was observed that with the same atomizers and burner geometry a substantial wider operation range was made possible. The only difference was the flame tube and the combustion chamber geometries. Therefore, it is recommended that selective geometrical changes to the flame tube (for enhancing recirculation rates) or to the burner should be made to achieve positive outcomes regarding reduction of the flame length and the emission of toxic pollutant gases.

In regard to the C30 MGT, the burner with the D_2 diameter is best qualified for the targeted improvements. Although the recorded flame lengths range from 90 mm to 115 mm, it poses little problem in terms of lack of space within the C30 combustion chamber since it incorporates an annular combustion chamber with an extended flame tube. Through the newly designed staging strategy notable exhaust gas emission improvement was realized.

7. ACKNOWLEDGMENTS

The authors would like to thank Mr. Jürgen Roth for his assistance with running the experiments and test rig operation. Special thanks to Mrs. Teresa Siebel for her efforts in designing the rest rig. This work was funded by Deutsches Zentrum für Luft- und Raumfahrt e.V. in the project "Next Generation Car – Antriebsstrang (NGS-AS)".

REFERENCES

[1] FLOX® is a registered trademark of WS Wärmeprozesstechnik GmbH, Renningen, Germany.

[2] Wünning, J. A., and Wünning, J. G. *Flameless Oxidation to Reduce Thermal NO–Formation*, 1997

[3] Lammel, O., et al. *FLOX® Combustion at High Power Density and High Flame Temperatures*. Journal of Engineering for Gas Turbines and Power, 132(12), p. 121503ff. 2010

[4] Severin, M. *Analyse der Flammenstabilisierung intensiv mischender Jetflammen für Gasturbinenbrennkammern*. Ph.D. dissertation, Institute of Combustion Technology for Aerospace Engineering (IVLR) University of Stuttgart. 2019

[5] Lefebvre, A. H., Ballal, D. R. *Gas Turbine Combustion*, 2010

[6] Panne, T. Charakterisierung numerischer Methoden für die Auslegung FLOX®-basierter Brennkammer-systeme. 2015

[7] Kislat, O. et al. *Detailed Experimental Investigation of the Operational Parameters of a 30 kW Micro Gas Turbine.* Proceedings of the ASME Turbo Expo 2019: Turbomachinery Technical Conference and Exposition. GT2019-90709. 2019

[8] Chen, J, et al. *Development of Ultra-Low Emission Diesel Fuel-Fired Microturbine Engines for Vehicular Heavy Duty Applications: Combustion Modification.* Proceedings of ASME Turbo Expo 2010: Power for Land, Sea and Air. GT2010-2318. 20101

[9] Gounder, J. D. et al. *Experimental and numerical investigation of spray characteristics in a new FLOX®–based combustor for liquid fuels for Micro Gas Turbine Range Extender (MGT-REX).* AIAA 2016

[10] Gokulakrishnan P. et al. *A Novel Low NO_x Lean, Premixed, and Prevaporized Combustion System for Liquid Fuels.* Journal of Engineering for Gas Turbines and Power SEPTEMBER 2008, Vol. 130 / 051501-1

[11] Weber R. et al. *On the (MILD) combustion of gaseous, liquid, and solid fuels in high temperature preheated air*. Proceedings of the Combustion Institute 30 (2005) 2623–2629. 2005

[12] Lee J. C. Y. et al. *Low NO_x Combustion for Liquid Fuels: Atmospheric Pressure Experiments Using a Staged Prevaporizer-Premixe.* Proceedings of: ASME TURBO EXPO 2001. 2001-GT-0081. 2001

[13] Cavaliere, A., Joannon, M., *Mild Combustion*, Prog. Energy Comb. Sci. 30, pp. 329-366: 2004

[14] Krishna, C. R. *Report on Atomization Tests for Project Titled "Biodiesel Blends in Microturbine".* Energy Sciences and Technology Department/Energy Resources Division. BNL-77928-2007-IR. 2007

[15] Izadi, S. *Characterization of Pressure Atomizers for a Single Nozzle Liquid FLOX® Burner Using Optical and Laser Diagnostics*. M.S. thesis, Institute of Combustion Technology for Aerospace Engineering (IVLR) University of Stuttgart. 2018

[16] Schäfer, D. *Untersuchung der Einflüsse verschiedener Zerstäuber auf die Leistung eines 2–Düsen–füssig–FLOX®–Brenners bei einem Betriebsdruck von 3,5 bar und einer Betriebstemperatur von 460 °C.* M.S. thesis, Institute of Combustion Technology for Aerospace Engineering (IVLR) University of Stuttgart. 2017

[17] Bolszo, C. et al. *Impact of Biodiesel on Fuel Preparation and Emissions for a Liquid Fired Gas Turbine Engine*. Proceedings of GT2007, ASME Turbo Expo 2007: Power for Land, Sea and Air. GT2007-27652. 2007

[18] Wei, Z. et al. *Optimization of Operating Parameters for Low NOxEmission in High-Temperature Air Combustion. Energy Fuels.* 26, 5, 2821-2829. 2012

[19] Nakamura1, S. et al. *The Effect of Liquid Fuel Preparation on Gas Turbine Emissions.* Journal of Engineering for Gas Turbines and Power. Vol. 130 / 021506-1. 2008

[20] Lammel, O., et al. *FLOX® Combustion at High Power Density and High Flame Temperatures.* Proceedings of ASME Turbo Expo 2010: Power for Land, Sea and Air. *GT2010-2338. 2010*

[21] Zanger, J. et al. *Experimental Investigation of the Combustion Characteristics of a Double-staged FLOX®–based Combustor on an Atmospheric and a Micro Gas Turbine Test Rig*. Proceedings of ASME Turbo Expo 2015: Turbine Technical Conference and Exposition. GT2015-42313. 2015

[22] Bower H. et al. *Experimental Analysis of a Micro Gas Turbine Combustor Optimized for Flexible Operation with Various Gaseous Fuel Compositions*. Proceedings of ASME Turbo Expo 2019: Turbomachines for Clean Power and Propulsion Systems. GT2019-90183. 2019

[23] Lee, J. G., and Santavicca, D. A., *Experimental Diagnostics for the Study of Combustion Instabilities in Lean Premixed Combustors*, J. Propul. Power 0748–4658 19, pp. 735–750, 2003

[24] Dandy, D. S., and Vosen, S. R. *Numerical and Experimental Studies of Hydroxyl Radical Chemiluminescence in Methane Air Flames*. Combustion Sci. Technol., 82, pp. 131 – 150. 1992

[25] Joos, F. *Technische Verbrennung - Verbrennungstechnik, Verbrennungsmodellierung, Emissionen*. Springer-Verlag Berlin Heidelberg. 2006

[26] Gounder, J. D., et al. *Spray Characteristics Measured in a New FLOX® Based Low Emission Combustor for Liquid Fuels Using Laser and Optical Diagnostics*. Proceedings of ASME Turbo Expo 2016: Turbomachinery Technical Conference and Exposition. GT2016-56629. 2016.

[27] Zizin, A., et al. *Development of a Jet-Stabilized Low-Emission Combustor For Liquid Fuels. Proceedings of ASME Turbo Expo* GT2015-42642. 2015

[28] Zanger, J., Zornek, T., Monz, T. *Entnahmesonde und Verfahren zur Entnahme von Abgas*. Patent reg. Nr.: DE 10 2017 102 046 A1 2018.08.02